THE JOURNAL OF PHYSICAL CHEMISTRY C
A JOURNAL OF THE AMERICAN CHEMICAL SOCIETY

pubs.acs.org/JPCC

Article

Identification of Impurity-Minimizing Synthesis Pathways for LAGP via Thermodynamic and Chemical Reaction Network-Based Analysis

Su Yeon Jang, Dong Won Jeon, Hyeon Woo Kim, Jin-Sung Park,* and Sung Beom Cho*

Cite This: *J. Phys. Chem. C* 2025, 129, 18433−18438

Read Online

ACCESS | Metrics & More | Article Recommendations

ABSTRACT: Solid-state synthesis is a widely used method for synthesizing various inorganic materials. However, impurity formation frequently occurs in multicomponent systems, making it challenging to achieve high phase purity. In this study, the cause of impurity formation in the synthesis of lithium aluminum germanium phosphate (LAGP, $Li_{1.5}Al_{0.5}Ge_{1.5}(PO_4)_3$), a NASICON-based solid electrolyte, was analyzed from a thermodynamic perspective. It was confirmed that when traditional precursors are used, impurities are inevitably generated as the reaction proceeds through multiple intermediate steps. To address this problem, a chemical reaction network (CRN)-based screening was performed to systematically identify alternative pathways that minimize impurity formation. Among a total of 95,620 possible reactions, no reaction could form phase-pure LAGP, and only 12 reactions produced GeO_2 as a byproduct, which is known to have minimal impact on ionic conductivity. Among these, two reactions were selected as candidate synthesis pathways and demonstrate the utility and scalability of CRN-based analysis in exploring complex reaction networks. This study presents an analytical framework that can be applied to a wide range of multicomponent inorganic systems as a strategy for designing high-purity solid-state synthesis routes.

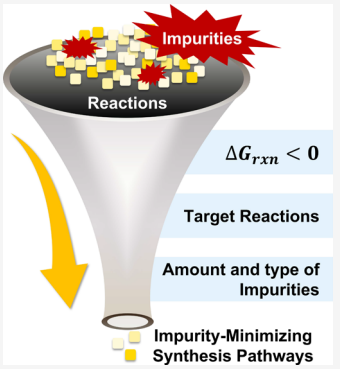

1. INTRODUCTION

Solid-state reaction synthesis is one of the most straightforward methods for preparing inorganic materials, owing to the wide availability of starting materials, ease of setup, and scalability.[1] This accessibility has driven significant advancements in various fields, such as batteries, piezoelectric materials, superconductors, and so on.[2−6] More recently, the inherent simplicity of this method has also acted as the foundation for the development of automated laboratories, which accelerate the discovery of new materials.[7] Despite these advantages, one of the main unresolved issues is the occurrence of impurities or undesired byproducts stemming from nonoptimized synthesis routes,[8] which becomes especially serious as materials expand toward multicomponent systems. While the demand for these functional materials continues to grow, the optimal synthesis pathway that consistently produces impurity-free materials remains elusive. This challenge persists mainly because the synthesis process typically relies on conventional precursors, such as binary compounds that may not favor the formation of the high-purity final product.[9−11] Therefore, attempts to explore novel approaches, such as modified precursor strategies or alternative reaction pathways, are imperative to develop synthesis routes that can minimize impurities and guarantee the quality of the finished product.

In this context, precursor engineering based on reaction pathfinding is emerging as a way to discover new optimal synthesis routes that can reduce impurities.[8−13] At its core, this methodology identifies the ideal thermodynamic conditions by exploring reactions that either maximize the driving force of the target product or minimize that of competing impurities across various precursor sets. Hence, determining the precise reaction pathway that leads to high-purity outcomes is crucial. However, finding an optimal synthesis route remains a significant challenge. First, the conventional synthesis pathways for a substantial number of materials remain unanalyzed, representing a 'black box'.[14,15] Since understanding these existing pathways is vital for estimating impurity-related purity, the lack of systematic data significantly hinders progress. Second, the sheer number of possible reactions to consider makes it overwhelming to find the optimal reaction routes. Even for ternary materials, there can be tens of thousands of potential reactions.[16,17] Moreover, as the number of components expands or the types of impurities increase, it becomes even more challenging. The lack of analytical data and the complexity of reactions hinder the application of optimal synthesis route discoveries to commercially functional materials, despite the demand for impurity reduction.

Received: June 19, 2025
Revised: September 26, 2025
Accepted: September 26, 2025
Published: October 3, 2025

https://doi.org/10.1021/acs.jpcc.5c04247
J. Phys. Chem. C 2025, 129, 18433−18438

A representative system that requires reaction route optimization is lithium aluminum germanium phosphate (LAGP), a NASICON-type solid electrolyte exhibiting lithium-ion conductivity on the order of $10^{-3}S \cdot cm^{-1}$ at room temperature.[18] In addition to its high ionic conductivity, LAGP exhibits excellent stability in air/water and favorable electrochemical stability, making it a promising candidate for solid-state batteries. Although LAGP can be synthesized via solid-state reactions using conventional binary precursors, it has long been[19] recognized as difficult to obtain in a phase-pure form due to the persistent formation of secondary phases. Even with advanced synthesis techniques such as coprecipitation, sol−gel processing, or spark plasma sintering, it remains inherently difficult to suppress the emergence of impurities such as $AlPO_4$, $Li_4P_2O_7$, Li_2O, and GeO_2.[18−29] These electrically insulating or refractory impurities are not just traces but structurally distinct phases. By interfering with particle-to-particle contact, they physically block ionic conduction paths, act as bottlenecks, and reduce the total ionic conductivity.[21] Therefore, the field now requires re-engineering of reaction pathways that thermodynamically prevent impurity formation and ensure phase-pure LAGP, going beyond simple adjustments of thermal profiles or experimental conditions.

In this study, we analyzed the traditional reaction pathways for LAGP to identify the origin of impurity formation and found a new optimal reaction route that addresses these challenges. First, we performed a thermodynamic exploration of the synthesis pathways to identify key factors and sources of the impurities. This process involved comparing interfacial energies to map the possible reaction pathways. Additionally, we proposed the optimal reaction that minimizes impurities by screening all reactions collected through the Chemical Reaction Network (CRN). This study proposes a method to effectively find the optimal synthetic route by overcoming the complexity of reactions for commercial functional materials.

2. METHODS

2.1. Crystal Structure. To accurately represent the disordered structure of $Li_3AlGe_3(PO_4)_6$ (LAGP), which is an alloy of $LiGe_2(PO_4)_3$ (LGP) doped with Al, we modeled the LAGP random alloy structures using Special Quasi-random Structures (SQS).[30] This modeling was performed with the mcsqs code provided in the Alloy Theoretic Automated Toolkit (ATAT). To create the LAGP model, we randomly replaced one of the four Ge^{4+} ion sites in LGP with an Al^{3+} ion and introduced an additional Li^+ ion to maintain electrical neutrality.[31]

2.2. Density Functional Theory Calculation. The DFT calculations were carried out using the Vienna Ab initio Simulation Package (VASP).[32,33] The projector-augmented wave (PAW) method was utilized to account for electron−ion interactions, and the generalized gradient approximation (GGA) within the Perdew−Burke−Ernzerhof (PBE) framework was applied for the exchange-correlation potential.[32] A cutoff energy of 520 eV was set for the calculations or structure optimization. The Hellmann−Feynman forces were converged to within 0.01 eV/Å, and the energy convergence criterion in the self-consistent field iteration was 10^{-5} eV for optimizations. For various analyses of LAGP computed by DFT, we integrated it with the Materials Project data and calibrated it using MaterialsProject2020Compatibility.[34]

2.3. Solid-State Reaction Energy. In solid-state synthesis, it is crucial to consider temperature when calculating the formation energy, as the scenarios being investigated occur at above room temperature. To account for the temperature dependence of the formation energy, the Gibbs free energy is expressed as

$$G_{formation}(T) = G_{product}(T) - G_{reactant}(T) \quad (1)$$

The entropy and enthalpy components, which contribute to the Gibbs free energy, are influenced by temperature. However, DFT-calculated values are temperature-independent, as they are determined at 0 K. Expressing the Gibbs free energy as a function of temperature, we have

$$G(T) = G^{\delta}(T) + \Delta H_f(298K) \quad (2)$$

To determine $G^{\delta}(T)$, we used a physical descriptor for the Gibbs energy of an inorganic crystalline solid using the SISSO method:[35,36]

$$G^{\delta}(T)\left[\frac{eV}{atom}\right] = (-2.48 \times 10^{-4} \times \ln(V) - 8.94 \times 10^{-5} mV^{-1})T + 0.181 \times \ln(T) - 0.882 \quad (3)$$

In this equation, V (Å^3/atom) denotes the atomic volume, m (amu) represents the reduced atomic mass, and T (K) is the temperature. Using this machine learning-based descriptor, the formation energy for each material was then computed at the synthesis temperature within a closed system. Additionally, the Gibbs reaction energy is calculated as follows:

$$G_{reaction} = \sum G_{products}(T) - \sum G_{reactants}(T) \quad (4)$$

2.4. Chemical Reaction Network. The Chemical Reaction Network (CRN) method is employed to trace the reaction path from the precursor to the final stage and monitor the associated energy changes by utilizing the formation of intermediates during the synthesis process.[16] CRN tracks all possible reactions in a system through reaction mechanisms between reactants at the interface and forms a complex network.

3. RESULTS

3.1. Thermodynamic Analysis of Traditional Solid-State Synthesis of LAGP. We first analyzed the traditional solid-state synthesis recipes for LAGP to investigate the existing reaction pathways. This analysis is necessary to simplify the actual synthesis process and effectively understand where impurities occur. Table 1 shows the conventional LAGP solid-state reaction recipes using commercial precursors and typical synthesis temperatures. The most commonly used precursors include Li_2CO_3 for Li source, Al_2O_3 for Al source,

Table 1. Traditional LAGP Solid-State Reaction Recipes Using Commercial Precursors

Commercial precursors	Synthesis temp	Heating time
[37] Li_2CO_3, Al_2O_3, GeO_2, $(NH_4)_2HPO_4$	900 °C	3h
[38] Li_2CO_3, Al_2O_3, GeO_2, $(NH_4)_2HPO_4$	900 °C	2h
[39] Li_2CO_3, Al_2O_3, GeO_2, $NH_4H_2PO_4$	1350 °C	1h
[40] Li_2CO_3, Al_2O_3, GeO_2, $(NH_4)_2HPO_4$	900 °C	6h
[41] Li_2CO_3, Al_2O_3, GeO_2, $NH_4H_2PO_4$	950 °C	10h

https://doi.org/10.1021/acs.jpcc.5c04247
J. Phys. Chem. C 2025, 129, 18433−18438

GeO_2 for Ge source, $(NH_4)_2HPO_4$, and $NH_4H_2PO_4$ for P source. These precursors typically react at temperatures between 900 and 1350 °C, depending on the heating time. It is known that when LAGP is synthesized according to these traditional solid-state reaction recipes, impurities such as $AlPO_4$, $Li_4P_2O_7$, Li_2O, and GeO_2 are formed.[18,38,41,42] However, the exact mechanism behind the formation of these impurities remains unclear and is often called a 'black box', as illustrated in Figure 1. To understand the origin of

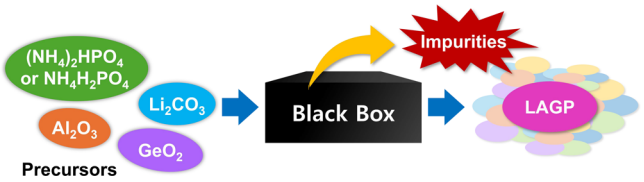

Figure 1. Schematic illustration of unknown reaction pathways and impurity formation in traditional LAGP synthesis using conventional precursors.

these impurities and address them, we initially performed a thermodynamic analysis of the synthesis reaction pathways. In solid-state synthesis, it is generally assumed that reactions tend to occur at the interface between precursor pairs with the highest reaction energy.[9,13] Based on this assumption, we determined the starting materials for the analysis by considering the melting points of conventional precursors. The conventional precursors for Li source, Al source, and Ge source have melting points of 723 °C (Li_2CO_3), 2072 °C (Al_2O_3), and 1115 °C (GeO_2), which are higher than or close to the synthesis temperature. In contrast, phosphorus sources required special attention because compounds such as $(NH_4)_2HPO_4$ and $NH_4H_2PO_4$ decompose to P_2O_5 at approximately 470 °C,[43] well below the typical synthesis temperature. Therefore, P_2O_5 was selected as the initial phosphorus source for the analysis, while the other elemental sources were chosen conventionally. This precursor set was then used to construct all possible pairwise interfacial reactions by comparing reaction energies, taking stoichiometry and quantitative balance into account.

Such pairwise interfacial reaction modeling has also been applied to other solid-state systems. For instance, in the synthesis of $YBa_2Cu_3O_6$, the reaction is known to initiate between CuO and BaO, forming $BaCuO_2$, driven by the strongest thermodynamic driving force at the interface. This is followed by a series of complex, multistep reactions, culminating in the reaction between the Ba−Cu−O compound and Y_2O_3 to synthesize $YBa_2Cu_3O_6$.[11] This example illustrates that solid-state synthesis typically proceeds through a sequence of interfacial reactions, beginning with those at the most thermodynamically favorable interfaces. Using this interface-driven approach, we analyzed the LAGP synthesis pathway by comparing interfacial reaction energies among conventional precursors, as summarized in Table 2. Accordingly, we found that the most reactive first reaction ($\Delta G_{rxn,925°C}$= −0.401 eV per atom) occurs between P_2O_5 and Al_2O_3, forming $AlPO_4$. Subsequently, the second reaction step was found to occur between GeO_2 and Li_2CO_3, producing Li_2GeO_3 ($\Delta G_{rxn,925°C}$= −0.156 eV per atom). It can be expected that the next step toward LAGP synthesis would be the reaction between $AlPO_4$ and Li_2GeO_3.

However, the reaction between Li_2GeO_3 and $AlPO_4$ proceeds through pathways with positive Gibbs free energies, such as

$$1.5Li_2GeO_3 + AlPO_4 \rightarrow Li_3AlGeO_5 + 0.5GeP_2O_7 (\Delta G_{rxn,925°C} = 0.109\text{eV per atom})$$

$$3Li_2GeO_3 + 2AlPO_4 \rightarrow Al_2Ge_2O_7 + 2Li_3PO_4 + GeO_2 (\Delta G_{rxn,925°C} = 0.030\text{eV per atom})$$

$$2Li_2GeO_3 + AlPO_4 \rightarrow LiAlGeO_4 + Li_3PO4 + GeO_2 (\Delta G_{rxn,925°C} = 0.013\text{eV per atom})$$

These reactions suggest that LAGP synthesis is thermodynamically unfavorable due to the energy barrier that prevents further spontaneous reactions. Nevertheless, LAGP synthesis has been experimentally achieved without significant difficulty. This suggests that the generated intermediates, as shown in Figure 2, may bypass the energy barrier by reacting with residual precursors to ultimately form LAGP.

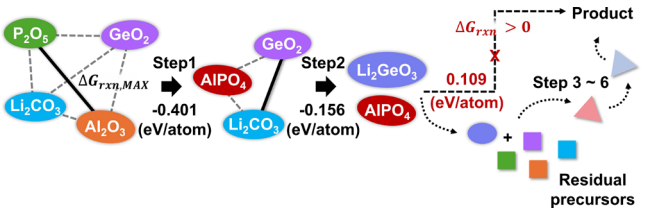

Figure 2. Thermodynamic analysis of the most probable LAGP synthesis pathway using traditional precursors with largest thermodynamic driving force, highlighting the energy barrier ($\Delta G_{rxn} > 0$) that hinders further progress.

Table 2. First-Step Interface Reactions among the Conventional Precursors in LAGP Synthesis

Reactants	Interface Reaction	$\Delta G_{rxn,925°C}$(eV/atom)
Li_2CO_3,Al_2O_3,GeO_2,P_2O_5	0.5 Li_2CO_3 + 0.5 Al_2O_3→ $LiAlO_2$ + 0.5 CO_2	−0.139
	Li_2CO_3 + GeO_2→ Li_2GeO_3 + CO_2	−0.156
	2 Li_2CO_3 + P_2O_5→ $Li_4P_2O_7$ + 2 CO_2	−0.314
	5 Al_2O_3 + 2 GeO_2→ $Al_{10}Ge_2O_{19}$	−0.019
	0.5 Al_2O_3+ 0.5 P_2O_5-→ $AlPO_4$	**-0.401**
	5 GeO_2 + 3 P_2O_5→ $Ge_5P_6O_{25}$	−0.107
$AlPO_4$,Li_2CO_3,GeO_2	$AlPO_4$ + 2 Li_2CO_3→ $LiAlO_2$ + Li_3PO_4 + 2 CO_2	−0.129
	Li_2CO_3+ GeO_2→ Li_2GeO_3+ CO_2	**-0.156**

https://doi.org/10.1021/acs.jpcc.5c04247
J. Phys. Chem. C 2025, 129, 18433−18438

Table 3. Reaction Steps to Synthesize LAGP by Avoiding Energy Barriers

Step	Reactants → Products	$\Delta G_{rxn,925°C}$(eV/atom)	Residual,Byproduct
Step 3	5 Li_2GeO_3 + 5.5 P_2O_5→ $Ge_5P_6O_{25}$ + 2.5 $Li_4P_2O_7$	−0.172	$Li_4P_2O_7$
Step 4	0.4 $Ge_5P_6O_{25}$ + 2.2 Al_2O_3→ $Al_2Ge_2O_7$ + 2.4 $AlPO_4$	−0.174	$AlPO_4$
Step 5 ∼ 6	0.5 $Al_2Ge_2O_7$ + 1.5 Li_2CO_3→ Li_3AlGeO_5 + 1.5 CO_2	−0.153	GeO_2
	Li_3AlGeO_5 + $Ge_5P_6O_{25}$→ LAGP + 3 GeO_2	−0.005	
	0.5 $Al_2Ge_2O_7$ + 0.5 Li_2CO_3→ $LiAlGeO_4$ + 0.5 CO_2	−0.108	$AlPO_4$
	3 $LiAlGeO_4$ + 4 P_2O_5→ LAGP + 2 $AlPO_4$	−0.167	

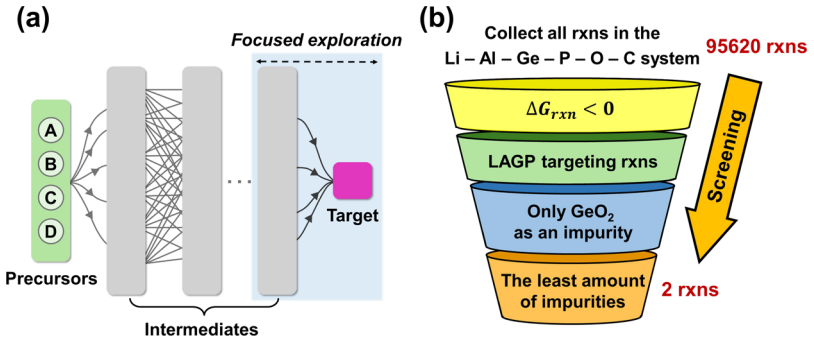

Figure 3. Suggestion of novel synthetic routes that can minimize impurities (a) Focus on reactions that can synthesize LAGP without generating unnecessary intermediates. (b) Workflow of the reaction screening with CRN.

Table 4. Impurity-Minimizing Reactions for LAGP Synthesis Identified through CRN-Based Screening, Generating Only GeO_2 as a By-product

Candidaterxns	Reactants → Products	$\Delta G_{rxn,925°C}$(eV/atom)
1	Li_3AlGeO_5+ 3 GeP_2O_7→LAGP + GeO_2	-0.017
2	2 $LiGe_2(PO_4)_3$+ $LiAlO_2$→LAGP + GeO_2	-0.020

To find a bypass pathway toward LAGP synthesis, it is necessary to examine the interfacial reaction energies between possible intermediates and the remaining precursors such as P_2O_5, Al_2O_3, Li_2CO_3, and GeO_2. We investigated the sequence of interfacial reactions through which Li_2GeO_3, an intermediate blocked by energy barriers, could lead to LAGP formation. Among all possible interfacial reactions, the reaction with P_2O_5 shows the largest thermodynamic driving force (5 Li_2GeO_3 + 5.5 P_2O_5 → $Ge_5P_6O_{25}$ + 2.5 $Li_4P_2O_7$, $\Delta G_{rxn,925\ °C}$= − 0.172 eV per atom). $Li_4P_2O_7$, one of the products formed in the above reaction, is blocked by a considerable energy barrier and cannot proceed further. On the other hand, $Ge_5P_6O_{25}$ reacts with Al_2O_3 to generate $Al_2Ge_2O_7$ and $AlPO_4$. Then, $Al_2Ge_2O_7$ reacts with Li_2CO_3 to form Li−Al−Ge-O compound, which then reacts with $Ge_5P_6O_{25}$ and P_2O_5 to produce the final product LAGP. The above analysis is summarized in Table 3, which shows that LAGP can be synthesized through a series of spontaneous interfacial reactions without thermodynamic energy barriers. However, the analysis also indicates that byproducts such as $AlPO_4$, $Li_4P_2O_7$, and GeO_2 are inevitably formed, which is consistent with previous reports on solid-state synthesis of LAGP.[18,38,41,42] In other words, when using existing commercial precursors, it is thermodynamically impossible to synthesize LAGP without byproducts, as numerous intermediates are formed during the reaction sequence and remain unreacted.

3.2. Reaction Screening for Optimal Synthesis Routes. We have found that impurities are inevitably formed due to numerous intermediate reactions when synthesizing LAGP in the solid state using commercial precursors. Therefore, we explored the optimal reaction routes that could proceed without intermediate reactions. To this end, we performed a reaction screening focusing on reactions that target LAGP, as illustrated in the region of interest in Figure 3(a). The screening process, as shown in Figure 3(b), begins by compiling all possible reactions at 925 °C in the Li−Al−Ge−P−O-C system, totaling 95,620 reactions. Next, we kept only the reactions with ΔG_{rxn} < 0 that could occur spontaneously, leaving 50,631 reactions. We then further narrowed the focus to reactions targeting LAGP, resulting in 99 reactions. At this stage, only reactions that can yield LAGP as a product without intermediate steps leading to impurities were selected. This subset accounts for only 0.2% of the overall reactions, demonstrating the large number of intermediate reactions when using conventional precursors.

In addition, none of the 99 reactions produced pure LAGP without impurities. This is likely because the formation of LAGP requires a delicate balance of five elements (Li, Al, Ge, P, and O) in a complex stoichiometric ratio, which makes it difficult to achieve a complete reaction without generating residual or side products. The impurities identified in the 99 reactions include $AlPO_4$ (36 reactions), Al_2O_3 (9 reactions), GeO_2 (12 reactions), and other byproducts such as $Li_4P_2O_7$, Li_3PO_4 and Li_2O (42 reactions combined). Among these impurities, $AlPO_4$ is known to significantly impair ionic conductivity by blocking Li-ion transport pathways.[21] While, as demonstrated by Chung et al., GeO_2 is considered to barely affect the ionic conductivity even though the amount increased as the excess of Li increased.[38] Therefore, from the 99 reactions with LAGP and impurities as products, we selected 12 that generated GeO_2 as the only byproduct. Among these 12, we propose two candidate reactions with the smallest

https://doi.org/10.1021/acs.jpcc.5c04247
J. Phys. Chem. C 2025, 129, 18433−18438

amounts of GeO_2 for the optimal synthesis route. The final candidate reactions, shown in Table 4, represent the optimal routes for LAGP synthesis with minimal impurities.

While direct experimental validation was not performed in this study, the optimal pathways identified through CRN-based screening appear to be practically feasible. These conclusions are supported by existing experimental literature. Specifically, the prediction that the reaction would form LAGP with GeO_2 as a byproduct is consistent with the experimental results of Pershina et al.[44] Their study confirmed that the target NASICON structure was produced with GeO2 as a minor impurity phase when using a similar set of elemental precursors, which aligns with our predictions. Furthermore, the precursor engineering strategy ensures the accessibility of the specific starting materials required for these pathways. For example, in the case of candidate reaction 2 listed in Table 4, $LiGe_2(PO_4)_3$ can be synthesized from Li_2CO_3, $(NH_4)H_2PO_4$, and GeO_2 as demonstrated by Fu et al.,[45] and $LiAlO_2$ is commercially available. The combination of these independent experimental studies strongly supports the practical feasibility of the optimal pathways identified by CRN. This demonstrates that the framework provides highly practical guidance for future experimental efforts to fundamentally suppress impurity formation and enable the synthesis of high-purity LAGP.

4. CONCLUSIONS

In this study, we investigated the origin of impurity formation in the solid-state synthesis of LAGP from a thermodynamic perspective. Our analysis confirmed that when conventional precursors are used, impurities are inevitably generated through intermediate reactions. To address this issue, we applied a CRN-based screening approach to systematically identify alternative reaction pathways that minimize impurity formation. Among 95,620 possible reactions, none were found to produce phase-pure LAGP. Only 12 reactions generated GeO_2 as a byproduct, which is known to barely affect ionic conductivity. Based on these findings, we proposed two optimal routes for LAGP synthesis, demonstrating that CRN-based screening can be effectively used to identify impurity-minimizing synthesis routes. The proposed synthesis pathways, guided by the precursor engineering strategy, demonstrate how CRN-based screening can be effectively used to identify impurity-minimizing synthesis routes. This framework has the potential to be extended as a design strategy for high-purity synthesis in a wide range of multicomponent solid-state systems.

AUTHOR INFORMATION

Corresponding Authors

Jin-Sung Park − *Department of Energy Systems Research and Department of Materials Science and Engineering, Ajou University, Suwon 16499, Republic of Korea*; Phone: (+82) 1052217564; Email: jinsung@ajou.ac.kr

Sung Beom Cho − *Department of Energy Systems Research and Department of Materials Science and Engineering, Ajou University, Suwon 16499, Republic of Korea*; orcid.org/0000-0002-3151-0113; Phone: (+82)1073041007; Email: csb@ajou.ac.kr

Authors

Su Yeon Jang − *Division of Chemical Engineering, Konkuk University, Seoul 05029, Republic of Korea; Department of Energy Systems Research, Ajou University, Suwon 16499, Republic of Korea*

Dong Won Jeon − *Department of Energy Systems Research and Department of Materials Science and Engineering, Ajou University, Suwon 16499, Republic of Korea*

Hyeon Woo Kim − *Department of Materials Science and Engineering, Ajou University, Suwon 16499, Republic of Korea*

Complete contact information is available at: https://pubs.acs.org/10.1021/acs.jpcc.5c04247

Notes

The authors declare no competing financial interest.

ACKNOWLEDGMENTS

Computational resources were supported by the Korea Supercomputing Center (No. KSC-2023-CRE-0387 and No. KSC-2024-CRE-0049). This work supported by the National R&D Program through the National Research Foundation of Korea (NRF) funded by the Ministry of Science and ICT (No. RS-2023-00209910), and Global-Learning & Academic Research Institution for Master & Ph.D. students, and Postdocs (LAMP) Program of the National Research Foundation of Korea (NRF) grant funded by the Ministry of Education (No. RS-2023-00285390).

REFERENCES

(1) Riedel, R.; Klapötke, T. M. *Synthesis of Inorganic Materials*, 4th ed.; Wiley-VCH, 2019.

(2) Padhi, A. K.; Nanjundaswamy, K. S.; Goodenough, J. B. Phospho-olivines as positive-electrode materials for rechargeable lithium batteries. *J. Electrochem. Soc.* **1997**, *144* (4), 1188−1194.

(3) Takenaka, T.; Kei-ichi Maruyama, K.-i. M.; Koichiro Sakata, K. S. (Bi1/2Na1/2)TiO3-BaTiO3 system for lead-free piezoelectric ceramics. *Jpn. J. Appl. Phys.* **1991**, *30*, 2236.

(4) Wu, M. K.; Ashburn, J. R.; Torng, C. J.; Hor, P. H.; Meng, R. L.; Gao, L.; Huang, Z. J.; Wang, Y. Q.; Chu, C. W. Superconductivity at 93 K in a new mixed-phase Y-Ba-Cu-O compound system at ambient pressure. *Phys. Rev. Lett.* **1987**, *58* (9), 908−910.

(5) Mizushima, K.; Jones, P. C.; Wiseman, P. J.; Goodenough, J. B. LixCoO2 (0x−1): A new cathode material for batteries of high energy density. *Mater. Res. Bull.* **1980**, *15* (6), 783−789.

(6) Nishida, N.; Miyatake, H.; Shimada, D.; Hikami, S.; Torikai, E.; Nishiyama, K.; Nagamine, K. Probing magnetism of high-Tc superconductor Y-Ba-Cu oxide by positive muons. *Jpn. J. Appl. Phys.* **1987**, *26* (5A), L799.

(7) Szymanski, N. J.; Rendy, B.; Fei, Y.; Kumar, R. E.; He, T.; Milsted, D.; McDermott, M. J.; Gallant, M.; Cubuk, E. D.; Merchant, A.; Kim, H.; Jain, A.; Bartel, C. J.; Persson, K.; Zeng, Y.; Ceder, G. An autonomous laboratory for the accelerated synthesis of novel materials. *Nature.* **2023**, *624* (7990), 86−91.

(8) Wang, Z.; Sun, Y.; Cruse, K.; Zeng, Y.; Fei, Y.; Liu, Z.; Shangguan, J.; Byeon, Y.-W.; Jun, K.; He, T.; Sun, W.; Ceder, G. Optimal thermodynamic conditions to minimize kinetic by-products in aqueous materials synthesis. *Nat. Synth.* **2024**, *3* (4), 527−536.

(9) Chen, J.; Cross, S. R.; Miara, L. J.; Cho, J.-J.; Wang, Y.; Sun, W. Navigating phase diagram complexity to guide robotic inorganic materials synthesis. *Nat. Synth.* **2024**, *3* (5), 606−614.

(10) Miura, A.; Bartel, C. J.; Goto, Y.; Mizuguchi, Y.; Moriyoshi, C.; Kuroiwa, Y.; Wang, Y.; Yaguchi, T.; Shirai, M.; Nagao, M.; Rosero-Navarro, N. C.; Tadanaga, K.; Ceder, G.; Sun, W. Observing and modeling the sequential pairwise reactions that drive solid-state ceramic synthesis. *Adv. Mater.* **2021**, *33* (24), No. e2100312.

(11) Bianchini, M.; Wang, J.; Clément, R. J.; Ouyang, B.; Xiao, P.; Kitchaev, D.; Shi, T.; Zhang, Y.; Wang, Y.; Kim, H.; Zhang, M.; Bai, J.; Wang, F.; Sun, W.; Ceder, G. The interplay between thermodynamics

and kinetics in the solid-state synthesis of layered oxides. *Nat. Mater.* **2020**, *19* (10), 1088−1095.
(12) He, T.; Huo, H.; Bartel, C. J.; Wang, Z.; Cruse, K.; Ceder, G. Precursor recommendation for inorganic synthesis by machine learning materials similarity from scientific literature. *Sci. Adv.* **2023**, *9* (23), No. eadg8180.
(13) McDermott, M. J.; McBride, B. C.; Regier, C. E.; Tran, G. T.; Chen, Y.; Corrao, A. A.; Gallant, M. C.; Kamm, G. E.; Bartel, C. J.; Chapman, K. W.; Khalifah, P. G.; Ceder, G.; Neilson, J. R.; Persson, K. A. Assessing thermodynamic selectivity of solid-state reactions for the predictive synthesis of inorganic materials. *ACS Cent. Sci.* **2023**, *9* (10), 1957−1975.
(14) Kohlmann, H. Looking into the black box of solid-state synthesis. *Eur. J. Inorg. Chem.* **2019**, *2019* (39−40), 4174−4180.
(15) Kim, W.; Kim, H. W.; Lee, H. U.; Kang, M. S.; Jeon, D. W.; Heo, S. W.; Cho, S. B. Predicting the synthesizability of double perovskite halides via interface reaction pathfinding. *Chem. Mater.* **2024**, *36* (12), 5904−5911.
(16) McDermott, M. J.; Dwaraknath, S. S.; Persson, K. A. A graph-based network for predicting chemical reaction pathways in solid-state materials synthesis. *Nat. Commun.* **2021**, *12* (1), 3097.
(17) Aykol, M.; Montoya, J. H.; Hummelshøj, J. Rational solid-state synthesis routes for inorganic materials. *J. Am. Chem. Soc.* **2021**, *143* (24), 9244−9259.
(18) DeWees, R.; Wang, H. Synthesis and properties of NaSICON-type LATP and LAGP solid electrolytes. *ChemSusChem.* **2019**, *12* (16), 3713−3725.
(19) Wang, Z.; Ma, Q.; Wu, Z.; Zhou, J.; Zhang, Q.; Zhang, Q.; Lv, P.; Yu, K.; Wei, W. Thermal and ionic conductivity improvement of LAGP glass ceramic and fiber thermal drawing. *Ceram. Int.* **2025**, *51* (7), 8615−8626.
(20) Kotobuki, M.; Hanc, E.; Yan, B.; Molenda, J.; Lu, L. Preparation and characterization of Ba-substituted Li1+xAlxGe2−x(PO4)3 (x = 0.5) solid electrolyte. *Ceram. Int.* **2017**, *43* (15), 12616−12622.
(21) Thokchom, J. S.; Kumar, B. The effects of crystallization parameters on the ionic conductivity of a lithium aluminum germanium phosphate glass−ceramic. *J. Power Sources.* **2010**, *195* (9), 2870−2876.
(22) Chowdari, B. V. R.; Subba Rao, G. V.; Lee, G. Y. H XPS and ionic conductivity studies on Li2O−Al2O3−(TiO2 or GeO2)−P2O5 glass−ceramics. *Solid State Ionics* **2000**, *136*, 1067−1075.
(23) Thokchom, J. S.; Kumar, B. Microstructural effects on the superionic conductivity of a lithiated glass-ceramic. *Solid State Ion.* **2006**, *177* (7−8), 727−732.
(24) Thokchom, J. S.; Kumar, B. Composite effect in superionically conducting lithium aluminium germanium phosphate based glass-ceramic. *J. Power Sources.* **2008**, *185* (1), 480−485.
(25) Yang, J.; Huang, Z.; Huang, B.; Zhou, J.; Xu, X. Influence of phosphorus sources on lithium ion conducting performance in the system of Li2O−Al2O3−GeO2−P2O5 glass−ceramics. *Solid State Ion.* **2015**, *270*, 61−65.
(26) Sun, S.; Cui, X.; Ma, Q.; Wang, J.; Ma, M.; Yao, X.; Cai, Q.; Li, J.; Chen, X.; Wang, Z.; Zhuang, R.; Mu, P.; Zhu, L.; Liu, J.; Yan, W. Insight into the role of crystallinity in oxide electrolytes enabling high-performance all-solid-state lithium-sulfur batteries. *J. Colloid Interface Sci.* **2023**, *650* (Pt A), 659−668.
(27) Lv, J.; Zheng, R.; Lv, P.; Wei, W. Effects of heat treatment and additive LiF on the properties of solid-state electrolyte of Li1.5Al0.5Ge1.5(PO4)3. *Energy Environ. Mater.* **2021**, *4* (2), 208−212.
(28) Markov, V.; Lebedeva, M.; Maximov, M.; Vishniakov, P. Effect of synthesis time and component excess on LAGP phase composition. In *2023 International Conference on Electrical Engineering and Photonics (EExPolytech)*; IEEE, 2023, pp. 320−323. DOI: .
(29) Kotobuki, M.; Koishi, M. Sol-gel synthesis of Li1.5Al0.5Ge1.5-(PO4)3 solid electrolyte. *Ceram. Int.* **2015**, *41* (7), 8562−8567.
(30) Zunger, A.; Wei, S.-H.; Ferreira, L. G.; Bernard, J. E. Special quasirandom structures. *Phys. Rev. Lett.* **1990**, *65* (3), 353−356.
(31) Weiss, M.; Weber, D. A.; Senyshyn, A.; Janek, J.; Zeier, W. G. Correlating transport and structural properties in Li1+xAlxGe2−x(PO4)3 (LAGP) prepared from aqueous solution. *ACS Appl. Mater. Interfaces.* **2018**, *10* (13), 10935−10944.
(32) Perdew, J. P.; Burke, K.; Ernzerhof, M. Generalized gradient approximation made simple. *Phys. Rev. Lett.* **1996**, *77* (18), 3865−3868.
(33) Kresse, G.; Furthmüller, J. Efficient iterative schemes for ab initio total-energy calculations using a plane-wave basis set. *Phys. Rev. B* **1996**, *54* (16), 11169−11186.
(34) Jain, A.; Hautier, G.; Ong, S. P.; Moore, C. J.; Fischer, C. C.; Persson, K. A.; Ceder, G. Formation enthalpies by mixing GGA and GGA + U calculations. *Phys. Rev. B* **2011**, *84* (4), No. 045115.
(35) Bartel, C. J.; Millican, S. L.; Deml, A. M.; Rumptz, J. R.; Tumas, W.; Weimer, A. W.; Lany, S.; Stevanović, V.; Musgrave, C. B.; Holder, A. M. Physical descriptor for the Gibbs energy of inorganic crystalline solids and temperature-dependent materials chemistry. *Nat. Commun.* **2018**, *9* (1), 4168.
(36) Ouyang, R.; Curtarolo, S.; Ahmetcik, E.; Scheffler, M.; Ghiringhelli, L. M. SISSO: a compressed-sensing method for identifying the best low-dimensional descriptor in an immensity of offered candidates. *Phys. Rev. Mater.* **2018**, *2* (8), No. 083802.
(37) Ling, S.-G.; Peng, J.-Y.; Yang, Q.; Qiu, J.-L.; Lu, J.-Z.; Li, H. Enhanced ionic conductivity in LAGP/LATP composite electrolyte. *Chin. Phys. B* **2018**, *27* (3), No. 038201.
(38) Chung, H.; Kang, B. Increase in grain boundary ionic conductivity of Li1.5Al0.5Ge1.5(PO4)3 by adding excess lithium. *Solid State Ion.* **2014**, *263*, 125−130.
(39) Feng, J. K.; Yan, B. G.; Liu, J. C.; Lai, M. O.; Li, L. All solid state lithium ion rechargeable batteries using NASICON structured electrolyte. *Mater. Technol.* **2013**, *28* (5), 276−279.
(40) Liu, Y.; Li, C.; Li, B.; Song, H.; Cheng, Z.; Chen, M.; He, P.; Zhou, H. Germanium thin film protected lithium aluminum germanium phosphate for solid-state Li batteries. *Adv. Energy Mater.* **2018**, *8* (16), No. 1702374.
(41) Inada, R.; Ishida, K.; Tojo, M.; Okada, T.; Tojo, T.; Sakurai, Y. Properties of aerosol deposited NASICON-type Li1.5Al0.5Ge1.5-(PO4)3 solid electrolyte thin films. *Ceram. Int.* **2015**, *41* (9), 11136−11142.
(42) Arbi, K.; Bucheli, W.; Jiménez, R.; Sanz, J. High lithium ion conducting solid electrolytes based on NASICON Li1+xAlxM2−x(PO4)3 materials (M = Ti, Ge and $0 \leq x \leq 0.5$). *J. Eur. Ceram. Soc.* **2015**, *35* (5), 1477−1484.
(43) Hao, J.; Du, Z.; Zhang, T.; Li, H. Influence of NH4H2PO4 powder on the laminar burning velocity of premixed CH4/air flames. *Int. J. Hydrogen Energy.* **2022**, *47* (90), 38477−38493.
(44) Pershina, S. V.; Il'ina, E. A.; Druzhinin, K. V.; Farlenkov, A. S. Effect of Li2O-Al2O3-GeO2-P2O5 glass crystallization on stability versus molten lithium. *J. Non-Cryst. Solids.* **2020**, *527*, No. 119708.
(45) Fu, J. Fast Li+ ion conducting glass-ceramics in the system Li2O−Al2O3−GeO2−P2O5. *Solid State Ion.* **1997**, *104* (3−4), 191−194.

https://doi.org/10.1021/acs.jpcc.5c04247
J. Phys. Chem. C 2025, 129, 18433−18438